

# High Dielectric Permittivity in $\text{AFe}_{1/2}\text{B}_{1/2}\text{O}_3$ Nonferroelectric Perovskite Ceramics (A - Ba, Sr, Ca; B - Nb, Ta, Sb)

I. P. Raevski<sup>1,2</sup>, S. A. Prosandeev<sup>1,3</sup>, A. S. Bogatin<sup>1</sup>, M. A. Malitskaya<sup>2,1</sup>

<sup>1</sup>*Physics Department, Rostov State University, 344090 Rostov on Don, Russia*

<sup>2</sup>*Research Institute of Physics, Rostov State University, 344090 Rostov on Don, Russia*

<sup>3</sup>*Ceramics Division, National Institute of Standards and Technology, Gaithersburg, MD*

(Dated: October 16, 2018)

$\text{AFe}_{1/2}\text{B}_{1/2}\text{O}_3$  (A - Ba, Sr, Ca; B - Nb, Ta, Sb) ceramics were synthesized and temperature dependencies of the dielectric permittivity were measured at different frequencies. The experimental data obtained show very high values of the dielectric permittivity in a wide temperature interval that is inherent to so-called high-k materials. The analyses of these data establish a Maxwell-Wagner mechanism as a main source for the phenomenon observed.

PACS numbers:

## I. INTRODUCTION

New perovskite-type materials exhibiting very high values of the dielectric permittivity  $\epsilon'$  in a very wide temperature interval discovered during last years open a new promising possibility for wide applications (the best known example is  $\text{CaCu}_3\text{Ti}_4\text{O}_{12}$  which has  $\epsilon'$  about 10000 which is nearly independent on temperature in the extremely wide temperature range, 100-500 K, both in ceramic and single crystal forms<sup>1,2,3,4</sup>). Such characteristics are of great interest for practice and several possible mechanisms have been already proposed<sup>2,3,4</sup>. At present it seems that the origin of the high dielectric permittivity is not intrinsic (as no anomalies in crystal lattice have been revealed by spectral and structural studies) but rather extrinsic, most probably- due to polarization of the Maxwell-Wagner type, but the origin and the scale of the concomitant electrical and/or chemical inhomogeneities are still under debate.

Recently high values of  $\epsilon'$  were reported for ceramic samples of ternary perovskite  $\text{BaFe}_{1/2}\text{Nb}_{1/2}\text{O}_3$  (BFN) and it was supposed that BFN is a relaxor ferroelectric ???. However, a close look into the temperature dependence of  $\epsilon'$  obtained in Ref. [5] and shown in Fig. 1 (dotted line), as well as the frequency dependencies of both the real  $\epsilon'$  and imaginary  $\epsilon''$  parts of dielectric permittivity resemble those observed for  $\text{CaCu}_3\text{Ti}_4\text{O}_{12}$ . This casts some doubts on the validity of the consequence made in Ref. [5] about the ferroelectric relaxor nature of the phenomenon observed.

The scope of the present work is the dielectric permittivity studies of  $\text{AFe}_{1/2}\text{B}_{1/2}\text{O}_3$  (A - Ba, Sr, Ca; B - Nb, Ta, Sb) in order to elucidate the nature of the high values of the dielectric permittivity in BFN and similar ceramics. For this purpose we also studied the electric field and temperature dependencies of electric current. We found out that all the ceramics studied exhibit large dielectric permittivity in a wide temperature interval and that a Maxwell-Wagner mechanism is responsible for these high values.

## II. EXPERIMENTAL

The ceramic samples of  $\text{AFe}_{1/2}\text{B}_{1/2}\text{O}_3$  were prepared by routine solid-state reaction route. The calculated quantities of appropriate carbonates and oxides were mixed thoroughly in an agate mortar in the presence of ethyl alcohol. Then the synthesis was carried out for 4 hours at 1000-1100 °C. After the synthesis the product of reaction was crushed and mixed in an agate mortar as described above. Usually 1wt.% of cubic boron nitride, BN, was added to the synthesized powder as a sintering aid. The green ceramic samples were pressed, at 100 MPa, in the form of disks of 5 to 10 mm in diameter and of 2-4 mm in height. Final sintering was carried out at 1200 – 1550°C. Pellets were placed on Pt foil. The density of the ceramics obtained was about 90-95 % of theoretical one. The absence of non-perovskite phases was monitored by X-ray diffraction. The electrodes for measurements were deposited to the grinded disk surfaces by rubbing the In-Ga alloy.

The dielectric studies were carried out in the 0.1-100 kHz range in the course of both heating and cooling at a rate of 2-3 °C/min with the aid of the R5083 capacitance bridge.

In order to avoid the Joule heating of the sample, volt-ampere characteristics of the semiconducting ceramics were studied by the pulse method with the aid of oscilloscope using the triangular-shaped voltage pulses.

## III. EXPERIMENTAL RESULTS

The resistivity  $\rho$  of ceramics obtained depends on the sintering temperature. The lowest  $\rho$  values  $\sim 10^3$ - $10^4 \text{ Ohm} \cdot \text{cm}$  were observed for  $\text{CaFe}_{1/2}\text{Nb}_{1/2}\text{O}_3$  ceramics sintered at  $T > 1300^\circ\text{C}$  while at lower sintering temperatures much higher  $\rho$  values were obtained. Other dielectric perovskite-type oxides usually have  $\rho \sim 10^7$ - $10^9 \text{ Ohm} \cdot \text{cm}$  at room temperature. The type of conductivity was determined by the Seebeck method for the most conductive samples and was found to be  $n$  for all

compounds studied.

The apparent  $\rho$  values of ceramics depend on the measuring field. Fig. 2 shows the dependences of current density  $j$  on the electric field  $E$  for three BFN ceramic samples having differing apparent  $\rho$  values at room temperature. At high  $E$ 's the  $j$  on  $E$  dependence is nonlinear and follows the  $j \sim E^\alpha$  relation where exponent  $\alpha$  varies from 3 to 5 for different samples. Such behavior is typical of ceramic varistors, i.e. ceramics with highly conducting grain bulk and poorly conducting grain boundary and/or intergranular layers [6,7]. Small  $\alpha$  values ( $\alpha < 1$ ) at low  $E$ 's are usually attributed to carriers hopping along the grain boundaries. It is worth noting that the same  $j$  vs.  $E$  curves may be fitted rather well by other types of dependences, e.g.  $j \sim \exp(aE^\nu)$  with  $\nu = 1$  or  $1/2$  etc. Various mechanisms of non-linear charge transport across the grain boundary barriers have been suggested for oxide semiconductors and are still under debate (see [6,7] and references therein). Discussions of these mechanisms is out of the scope of the present work. It is only essential for us that our experiment shows that the ceramics under study are electrically inhomogeneous.

One more important conclusion follows from the large values of  $E$  corresponding to the onset of the highly-nonlinear portions of the  $j(E)$  dependences. This fact implies that the samples studied contain a large number of high-resistive layers and the role of possible blocking layer at the sample/electrode interface is negligible. Qualitatively similar  $j(E)$  dependencies were observed for all the  $\text{AFe}_{1/2}\text{B}_{1/2}\text{O}_3$  ceramics studied provided that the samples have low enough apparent resistivity.

Fig. 1 displays the  $\varepsilon'(T)$  and  $\tan\delta(T)$  dependences for three BFN samples having differing apparent resistivity at room temperature (see Table 1). As both  $\varepsilon'$  and  $\tan\delta$  change by several orders of magnitude the semilogarithmic scale is used. The  $j(E)$  dependences for BFN-1 and BFN-2 samples are similar to curves 2 and 3 in Fig.2 respectively, while no highly-nonlinear portions were observed on the  $j(E)$  dependence of the BFN-3 sample in the available range of  $E$  values (up to 300 V/mm).

All the  $\varepsilon'(T)$  dependences obtained are similar to those observed for the so-called high-k materials<sup>1,2,3,4,8</sup>:  $\varepsilon'(T)$  has a step and, above the temperature of this step,  $\varepsilon'$  are nearly independent on  $T$ . Only at high temperatures one can see a small increase of  $\varepsilon'$ .

The BFN-1 and BFN-2 samples have very similar  $\varepsilon'$  values and  $\varepsilon'(T)$  dependences;  $\tan\delta$  of BFN-1 is somewhat higher with respect to BFN-2, especially at room temperature and above (Fig. 1). These higher  $\tan\delta$  values may be attributed to higher apparent conductivity of BFN-1.

Both the  $\varepsilon'(T)$  steps and  $\tan\delta(T)$  maxima shift to higher temperatures as the measuring frequency,  $f$ , increases (Figs. 3 and 4). Both the  $\varepsilon'(T)$  and  $\tan\delta(T)$  maximum temperature,  $T_m$ , dependences on  $f$  plotted in the Arrhenius coordinates are linear (Fig. 4) which is typical of Debye-type relaxation. The activation energies  $\Delta E_f$  determined from either of these

dependences are very similar (Fig. 4).

As temperature decreases,  $\varepsilon'(T)$  curves of all the three BFN samples tend to converge. From our data the low-temperature limit of  $\varepsilon'$  may be estimated as 40-60. This value seems to be somewhat lower if the measurements would be extended to lower temperatures and/or higher frequencies. The high-frequency value of  $\varepsilon'$  for BFN is close to the estimate  $\varepsilon' \approx 22$  obtained using the linear correlation between the  $\varepsilon'$  values measured in the submillimeter frequency range and tolerance-factor  $t = (R_A + R_B)/\sqrt{2}(R_B + R_O)$ , revealed for  $\text{A}^{2+}\text{B}_{1/2}^{3+}\text{B}_{1/2}^{5+}\text{O}_3$  perovskites<sup>9</sup> ( $R_A$ ,  $R_B$  and  $R_O$  stand for the ionic radii of the A, B and O ions respectively).

Fig. 5 shows the  $\varepsilon'(T)$  and  $\tan\delta(T)$  dependences for several  $\text{A}^{2+}\text{Fe}_{1/2}\text{B}_{1/2}\text{O}_3$  ceramics. These curves as well as the Arrhenius plots of the frequency dependence of the  $\tan\delta(T)$  maximum temperature (Fig.6) are very much alike the corresponding dependences for BFN. For all the  $\text{A}^{2+}\text{Fe}_{1/2}\text{B}_{1/2}\text{O}_3$  perovskites studied the low-temperature values of  $\varepsilon'$  are close to that of BFN ceramics. Note that the temperature at which the  $\varepsilon'(T)$  step is observed and the activation energy of relaxation depend on the apparent resistivity values of the samples. Such behavior is typical of the Maxwell-Wagner relaxation and below we shall give some additional arguments in favour of this conclusion.

#### IV. DISCUSSION

In the simplest version of the Maxwell-Wagner relaxation model one can consider alternating slabs having different dielectric permittivities ( $\varepsilon_1$  and  $\varepsilon_2$ ) and different conductivities ( $\sigma_1$  and  $\sigma_2$ ), so that the complex permittivities in these slabs are:

$$\begin{aligned}\varepsilon_1^* &= \varepsilon_1 - i\sigma_1/\omega \\ \varepsilon_2^* &= \varepsilon_2 - i\sigma_2/\omega\end{aligned}\quad (1)$$

At small conductivities the total dielectric permittivity can be approximated by

$$\varepsilon^* = \frac{L}{l\varepsilon_1^{*-1} + d\varepsilon_2^{*-1}}\quad (2)$$

where  $l$  and  $d$  are the widths of the first and second slabs respectively, and  $L = l + d$ .

Then we consider expression (2) where, for the sake of simplicity, only the first slab is conducting. This slab corresponds to the grain bulk while the nonconducting slab is the grain boundary. We assume that the temperature dependence of electroconductivity in the conducting grains is semiconducting

$$\sigma_1 = \sigma_{10}e^{-\Delta E_\sigma/k_B T}\quad (3)$$

where  $\Delta E_\sigma$  is the electroconductivity activation energy (this energy can vary for different samples depending on the degree of the donor-acceptor compensation). This assumption corresponds to our experimental data on electroconductivity.

Equating  $l$  and  $L$  (this is true for thin interfacial layers between grains) one can obtain

$$\varepsilon^* = \frac{\varepsilon_1}{a} + \frac{\varepsilon_2}{a\delta} \frac{1}{1 + i\omega\tau} \quad (4)$$

where  $a = 1 + \delta\varepsilon_1/\varepsilon_2$ ,  $\tau = \varepsilon_2 a / \delta\sigma_1$ , and  $\delta$  being the relative width of the interfacial layers  $\delta = d/L$ . The frequency dependence of the dielectric permittivity can be observed if only  $a\delta \ll \varepsilon_2$ . This can happen in the case if the nonconductive layers are very thin that corresponds to our assumption about the grain boundaries, and if the dielectric permittivity of the conductive region is not very large with respect to the nonconductive one, and this also corresponds to our data showing comparatively (with ferroelectrics) low values of the permittivity at low temperatures and large frequencies.

At zero frequency one can find

$$\varepsilon' = L\varepsilon_2/d \quad (5)$$

that is the dielectric permittivity is controlled by the thin nonconducting layer. In the case of ceramics considered in the present paper this can be boundaries of the grains. For example, if the grain is about 10  $\mu\text{m}$ , the boundary region is about 100 Å, and  $\varepsilon_2 = 20$  then  $\varepsilon' = 20000$ . This can explain the high values of the dielectric permittivity in BFN. For instance, at  $\varepsilon_1 = 40$ , one can obtain the high frequency limit  $\varepsilon' = 40$  which corresponds to our experimental data.

It follows from (4) that the temperature dependence of the relaxation time  $\tau$  can be described by the Arrhenius law, in which the barrier height coincides with the electroconductivity activation energy in the grain's bulk:

$$\tau = \tau_0 e^{\Delta E_\sigma / k_B T} \quad (6)$$

where  $\tau_0 = a/\delta\sigma_{10}$ . This fact corresponds to the experimental data showing a close relation of the electroconductivity in the bulk of the grains to the relaxation time (see Section 3). Due to temperature dependence (6) the real part of the dielectric permittivity should increase at a temperature determined by the relation  $\omega\tau \approx 1$  and at larger temperatures it should saturate that is in agreement with experiment. The greater is the frequency, the larger is the temperature where the real part of the permittivity becomes rapidly growing and the imaginary part has a maximum. These data are in excellent agreement with the experiment performed.

The microscopic model we use bases on the assumption that the high-temperature treatment of the ceramics under study results in the creation of oxygen vacancies

which have weakly bound electrons. The semiconductor conductivity connected with these electrons contributes into electric polarization and results in the appearance of a step in  $\varepsilon'$  and a maximum in  $\varepsilon''$ .

We assumed that the interfacial layers at the grain boundaries are nonconducting (or less conducting) while the bulk of the grains is conducting. Just this fact together with the relatively small total width of the grain boundaries in the direction of the field provides the large values of the dielectric permittivity in the ceramics studied.

Both the resistivity dependence on sintering temperature and varistor-like  $j(E)$  characteristics of the  $\text{AFe}_{1/2}\text{B}_{1/2}\text{O}_3$  ceramics seem to be due to partial reduction of these compounds at high temperatures (where the partial  $\text{O}_2$  pressure in air is lower than the equilibrium partial  $\text{O}_2$  pressure in oxide). This assumption is consistent with the  $n$ -type of conductivity in all the ceramics studied. In the course of cooling reoxidation takes place. As the oxygen diffusion coefficient at grain boundaries is much larger than in the bulk, the degree of oxidation and subsequent resistivity is higher in the grain boundary layers than in the grain bulk.

As one can see from Table 1, the activation energies of the relaxation frequency are several times lower than the activation energies extracted from the temperature dependence of  $\rho$ . The former energy coincides with the activation energy of grain bulk conductivity (see expression (6)) while the latter is determined by the grain boundary barrier height. The same situation is observed in  $\text{CaCu}_3\text{Ti}_4\text{O}_{12}$  ceramics where the resistivities of grain bulk and grain boundaries have been directly determined via the impedance spectroscopy [4]. It is worth noting that the activation energies observed for the relaxation time have the same order of magnitude as the activation energies of the first (hundredths of eV) and the second (tenths of eV) levels of the oxygen vacancy in perovskites [10,11].

Similar effects, i.e. a crucial dependence of resistivity on sintering temperature and the formation of grain boundary barrier layers due to reoxidation have been observed in related compounds  $\text{PbFe}_{1/2}\text{Nb}_{1/2}\text{O}_3$  and  $\text{PbFe}_{1/2}\text{Ta}_{1/2}\text{O}_3$ <sup>12,13,14</sup>. Both these perovskites are ferroelectrics and the presence of grain boundary barriers in a ceramic sample can be monitored by studying the positive temperature coefficient of resistivity (PTCR) effect, an anomalous decrease of resistivity on cooling below the ferroelectric Curie point,  $T_C$ . In the paraelectric phase the properties of these materials at low frequencies are determined mainly by grain boundaries: the extremely high permittivity values (though depending on temperature due to the Curie-Weiss behavior of  $\varepsilon'$  typical of ferroelectrics), varistor effect, and high apparent resistivity exhibiting large activation energy were observed. Below  $T_C$ , the grain boundary barriers are screened, more or less effectively, due to onset of the spontaneous polarization. This results in low resistivity values characterized by small activation energies which are determined by the

grain bulk and relatively small residual grain boundary barriers.

The average grain size in all the BFN ceramics studied was approximately the same (a few  $\mu\text{m}$ ) and the increase of the  $E$  values corresponding to the onset of the highly-nonlinear portions on the  $j(E)$  curves of the samples with lower apparent conductivity is likely to be caused by the increase of the thickness of the poorly conducting grain boundary layers. This assumption correlates well (taking into account expression (5)) with experimentally observed lower values of  $\epsilon'$  for the BFN-3 sample as compared with more conductive BFN-2 and BFN-1.

It follows from expressions (4) and (6) that the temperature behavior of  $\tan \delta$  can have whether a maximum (at low frequency or at high conductivity) or a step (at large frequency or at low conductivity). There can be also intermediate behavior with a step and a maximum just at the step. This corresponds to the experiment performed as it is seen from Figs. 1 and 6.

Fig. 7 presents the fit of expression (4) to experimental data obtained for BFN2. The activation energy of the relaxation process obtained from this fit is 0.09 eV that is in excellent agreement with the experimental data obtained from the Arrhenius plot.

We want to stress here that the Debye-type relaxation described above differs from the usual Debye relaxation connected with the reversal of local dipoles appreciably. In the case of the local dipoles  $\epsilon(\omega = 0) \sim 1/T$  and this explains the vanishing of the relaxation contribution to the dielectric permittivity at high temperatures. The real part of the dielectric permittivity in this case has a maximum and the temperature width of the relaxation anomaly is usually not very large. We expect such a situation for low-conducting samples where the conducting regions are so small that one cannot substitute the complex system by a series of capacitors. Rather simple arithmetic averaging of dielectric permittivity should be done. In this case one immediately obtains a Lanjevin function describing polarization, and, at zero measuring field, the permittivity is  $\chi_0 \approx nd^2e/6k_B T$  where  $d$  is the width of the polar region along the field,  $e$  is the electron charge, and  $n$  is the oxygen vacancy concentration. Notice that this result is obtained not because of the averaging of polarization over the possible dipole directions in 3D space as it is true for local dipoles but rather because of averaging of polarization with respect to the displacement of an electron from the oxygen vacancy along the field. The real part of the dielectric permittivity has a maximum in this case like in the case of local dipoles and the susceptibility decreases with temperature above the maximum as  $1/T$ .

We have considered a monodispersive Debye model. However it can be easily generalized by considering a distribution function of the relaxation times. There can be a few relaxation processes connected with different electron's states. They can lead to different maximums or steps in the imaginary part of permittivity in different temperature intervals. The spatial dependence of the

parameters of the model can be taken into account by introducing a distribution function for the relaxation times and energy barriers.

We want to discuss here a possibility of the existence of a Maxwell-Wagner relaxation in single crystals. Indeed, such relaxation was observed in single crystals of  $\text{CaCu}_3\text{Ti}_4\text{O}_{12}$ [1,2] and  $\text{ErFe}_2\text{O}_4$  <sup>8</sup>. In principle this effect could be due to electrodes and a depletion region near them. In our case we used InGa electrodes which do not produce such an effect in the case of the n-type conductivity found in our samples. Another possibility can be connected with the fact that all high-k materials contain transition metal ions with open shells like Fe (in our case and in  $\text{ErFe}_2\text{O}_4$ ) or Cu (in  $\text{CaCu}_3\text{Ti}_4\text{O}_{12}$ ). Below we will discuss a few of possible consequences of this fact.

The oxygen vacancies are comparatively easily created at the transition metals in perovskites and they are ordered<sup>15</sup>. This can result in the appearance of reduced regions in the bulk at the transition metals and these regions can organize clusters and participate in the conductivity. The ordered arrays of the vacancies can play the role of conducting layers.

The electronic band structure of  $\text{AFe}_{1/2}\text{B}_{1/2}\text{O}_3$  (A-Ba,Sr,Ca; B-Nb,Ta,Sb) is very different in comparison with the electronic structure of  $\text{ABO}_3$  perovskites<sup>16</sup>. Indeed the width of conduction bands in the  $\text{ABO}_3$  crystals is mainly determined by the covalent bonding of the  $nd$  metal and  $\text{O}2p$  oxygen electronic states. At the Fe ions the covalent bonding is reduced due to the localized character of the Fe  $3d$ -states. This effect should decrease the width of the conduction bands [16] and produce some percolative clusters made of conducting states. The electrons from the vacancies caught by these clusters can participate in charge transfer within these clusters. The charges of  $\text{Fe}^{3+}$  and  $\text{B}^{5+}$  (B - Nb, Ta, Sb) are very different, and this also can lead to the appearance of clusters of electronic conduction states having decreased energy. One can consider conductivity percolation in samples after different thermal treatment: for well conductive samples the percolative clusters are big while for less conductive clusters they are smaller.

Finally, one can consider electron's jumps over the M-O bands (M = Cu or Fe). Due to a small oxygen vacancy concentration this conductivity is prevented by the strong electron correlation on the metal ions. As a result the electrons can be caught by some finite regions having random barriers which are higher than the barriers inside these volumes.

In Ref. [8] the authors proposed the appearance of nonconducting (or less conducting) layers due to a magnetic phase transition and following domain formations: the domain walls can play the role of the nonconducting dielectric layers. One can extend this idea by considering also antiferroelectric or elastic phase transitions.

Studies of the electron doping on the dielectric properties of perovskite materials were carried out in pioneering papers<sup>19,20,21</sup>. It was not ambiguously shown that elec-

trons and polarons can contribute much to the dielectric permittivity of perovskites and, at some conditions, produce a temperature maximum of the dielectric permittivity. From our study it follows that such "polaronic-type" relaxation is possible in the case when the polar regions where the electron concentration is enhanced for some reasons are not very large. In this case these regions show the same characteristics as local orientable dipoles in relaxors.

## V. SUMMARY

Experiments performed have shown that ceramics  $\text{AFe}_{1/2}\text{B}_{1/2}\text{O}_3$  (A - Ba, Sr, Ca; B - Nb, Ta, Sb) have similar main features in the temperature dependence of dielectric permittivity:  $\epsilon'$  has a large step in the interval between  $-100^\circ\text{C}$  and  $100^\circ\text{C}$ , the magnitude of  $\epsilon'$  is low below the step (less than  $10^2$ ) and large above the step (of the order of  $10^3$ -  $10^4$ ); the large value of  $\epsilon'$  remains above the step in the whole temperature interval studied;  $\tan\delta$  has a maximum or also a step with a small maximum;  $\epsilon'$  and  $\tan\delta$  depend on frequency: the respective step and maximum are shifted to higher temperatures at larger frequencies, while the magnitude of the permit-

tivity at the maximal value of the step does not change much. All these features were found to be influenced by the conductivity of the samples: in the samples with higher conductivity the step lays at lower temperatures and the maximal value of  $\epsilon'$  is higher.

We propose that the phenomenon of the high values of the dielectric permittivity in ceramics  $\text{AFe}_{1/2}\text{B}_{1/2}\text{O}_3$  (A - Ba, Sr, Ca; B - Nb, Ta, Sb) in a wide temperature interval is due to the Maxwell-Wagner relaxation. We fitted an expression of this model to the experimental data and found reasonable agreement between the theory and experiment. It seems that a  $\epsilon'(T)$  step-like anomaly reported for  $\text{SrFe}_{1/2}\text{Sb}_{1/2}\text{O}_3$  at  $\approx 220\text{K}$  and attributed to the presence of an antiferroelectric phase transition<sup>17</sup> is due to the Maxwell-Wagner relaxation. The same seems to be the case for  $\text{SrTiO}_3:\text{Bi}$ <sup>18</sup> as well as for  $\text{CaCu}_3\text{Ti}_4\text{O}_{12}$ <sup>1,2,3,4</sup>.

## VI. ACKNOWLEDGEMENTS

This work was partially supported by Russian Foundation for Basic Research (Grants 01-03-33119 and 01-02-16029).

- 
- <sup>1</sup> M. A. Subramanian, D. Li, N. Duan, B. A. Reisner and A. W. Sleight, *J. Solid State Chem.* **151**, 323 (2000).
- <sup>2</sup> C. C. Homes, T. Vogt, S. M. Shapiro, S. Wakimoto, and A. P. Ramirez, *Science* **293**, 673 (2001).
- <sup>3</sup> L. He, J. B. Neaton, M. H. Cohen, D. Vanderbilt and C. C. Homes, *Phys. Rev. B* **65**, 214112 (2002).
- <sup>4</sup> D. C. Sinclair, T. B. Adams, F. D. Morrison and A. R. West, *Appl. Phys. Lett.* **80**, 2153 (2002)
- <sup>5</sup> S. Saha and T. P. Sinha, *Phys. Rev. B* **65**, 134103 (2002).
- <sup>6</sup> Clarke D. R. *J. Amer. Ceram. Soc.* **82**, 485 (1999).
- <sup>7</sup> I. P. Raevski and A. N. Pavlov, *Zh. Tekh. Fiz.* **67**, 21 (1997) (In Russian). [English translation: *Tech. Phys.* **42**, 1390 (1997)].
- <sup>8</sup> N. Ikeda, K. Kohn, H. Kito, J. Akimitsu and K. Siratori, *J. Phys. Soc. Jap.* **64**, 1371 (1995).
- <sup>9</sup> R. Zurmuhlen, J. Petzelt, S. Kamba, G. Kozlov, A. Volkov, B. Gorshunov, D. Dube, A. Tagantsev and N. Setter, *J. Appl. Phys.* **77**, 5351 (1995).
- <sup>10</sup> S. A. Prosandeyev, A. V. Fisenko, A. I. Riabchinskii et al. *J. Phys.: Condens. Matter* **8**, 6705 (1996).
- <sup>11</sup> I. P. Raevski, S. M. Maksimov, A. V. Fisenko, S. A. Prosandeyev, I. A. Osipenko, and P. F. Tarasenko, *J. Phys.: Condens. Matter* **10**, 8015 (1998).
- <sup>12</sup> I. P. Raevski, M. A. Malitskaya, V. P. Filippenko, O. I. Prokopalo, A. N. Pavlov and E. I. Bondarenko, *Fiz. Tverd. Tela (Leningrad)* **28**, 3211 (1986) (In Russian) [English translation: *Phys. Solid State* **28**, 1811 (1986)].
- <sup>13</sup> I. P. Raevski, M. A. Malitskaya, V. P. Filippenko, O. I. Prokopalo, L. P. Bashkurova and L. G. Kolomin, *Zh. Tekh. Fiz.* **58**, 1196 (1988) (In Russian)
- <sup>14</sup> I. P. Raevski, M. A. Malitskaya, S. A. Trusova and L. G. Kolomin, *Fiz. Tverd. Tela (St. Petersburg)* **35**, 856 (1993) (In Russian) [English translation: *Phys. Solid State* **35**, 444(1993)].
- <sup>15</sup> J. F. Scott, *Ferroelectric Memories*, Vol. 3 of *Advanced Electronics*, Springer, Heidelberg, 2000.
- <sup>16</sup> I. P. Raevskii, S. A. Prosandeev, and I. A. Osipenko, *Phys. Stat. Sol. (b)* **198**, 695 (1996).
- <sup>17</sup> E. D. Politova, I. N. Danilenko and Yu. N. Venevtsev, *Ferroelectrics* **81**, 1209 (1988).
- <sup>18</sup> C. Ang, Z. Yu and L. E. Cross, *Phys. Rev. B* **62**, 228 (2000).
- <sup>19</sup> M. Maglione and M. Belkaoui, *Phys. Rev. B* (45), 2029 (1992).
- <sup>20</sup> O. bidault, M. Maglione, M. Actis, M. Kchikech, and B. Salce, *Phys. rev. B* **52**, 4191 (1995).
- <sup>21</sup> O. Bidault, P. Goux, M. Kchikech, M. Belkaoui, and M. Maglione, *Phys. Rev. B* **49**, 7868 (1994).

TABLE I: Apparent resistivity,  $\rho$ , at room temperature, and activation energies  $\Delta E_f$  and  $\Delta E_\rho$  for  $\text{AFe}_{1/2}\text{B}_{1/2}\text{O}_3$  ceramics and  $\text{CaCu}_3\text{Ti}_4\text{O}_{12}$  <sup>4</sup>

Compound	$\rho$ [Ohm · cm]	$\Delta E_f$ [eV]	$\Delta E_\rho$ [eV]
$\text{BaFe}_{1/2}\text{Nb}_{1/2}\text{O}_3$ (BFN-1)	$\sim 10^7$	0.08	0.3
$\text{BaFe}_{1/2}\text{Nb}_{1/2}\text{O}_3$ (BFN-2)	$\sim 10^8$	0.08	0.3
$\text{BaFe}_{1/2}\text{Nb}_{1/2}\text{O}_3$ (BFN-3)	$\sim 10^9$	0.35	0.55
$\text{BaFe}_{1/2}\text{Nb}_{1/2}\text{O}_3$ [ 5 ]	$\sim 10^8$	0.12	
$\text{BaFe}_{1/2}\text{Ta}_{1/2}\text{O}_3$	$\sim 10^8$	0.08	0.4
$\text{SrFe}_{1/2}\text{Nb}_{1/2}\text{O}_3$	$\sim 10^8$	0.16	0.4
$\text{CaFe}_{1/2}\text{Nb}_{1/2}\text{O}_3$	$\sim 10^9$	0.3	0.7
$\text{SrFe}_{1/2}\text{Sb}_{1/2}\text{O}_3$	$\sim 10^9$	0.4	0.7
$\text{CaCu}_3\text{Ti}_4\text{O}_{12}$ <sup>4</sup>		0.08	0.6

### Figure captions

Fig. 1. Temperature dependencies of  $\varepsilon'$  (upper curves) and  $\tan\delta$  (lower curves) measured at 1 kHz for three BFN1 (1), BFN2 (2), and BFN3 (3) (see notations in Table 1). The dashed line shows the  $\varepsilon'(T)$  dependence for a BFN ceramics deduced from Ref. [5].

Fig. 2. Typical logarithmic plots of  $j(E)$  for BFN ceramic samples having different apparent resistivity at room temperature. The upper curve corresponds to a

more conductive sample with  $\rho \sim 10^7 \text{Ohm} \cdot \text{cm}$  while the lower curve is for a less conductive sample with  $\rho \sim 10^9 \text{Ohm} \cdot \text{cm}$ . The dashed line shows an Ohm-type behavior.

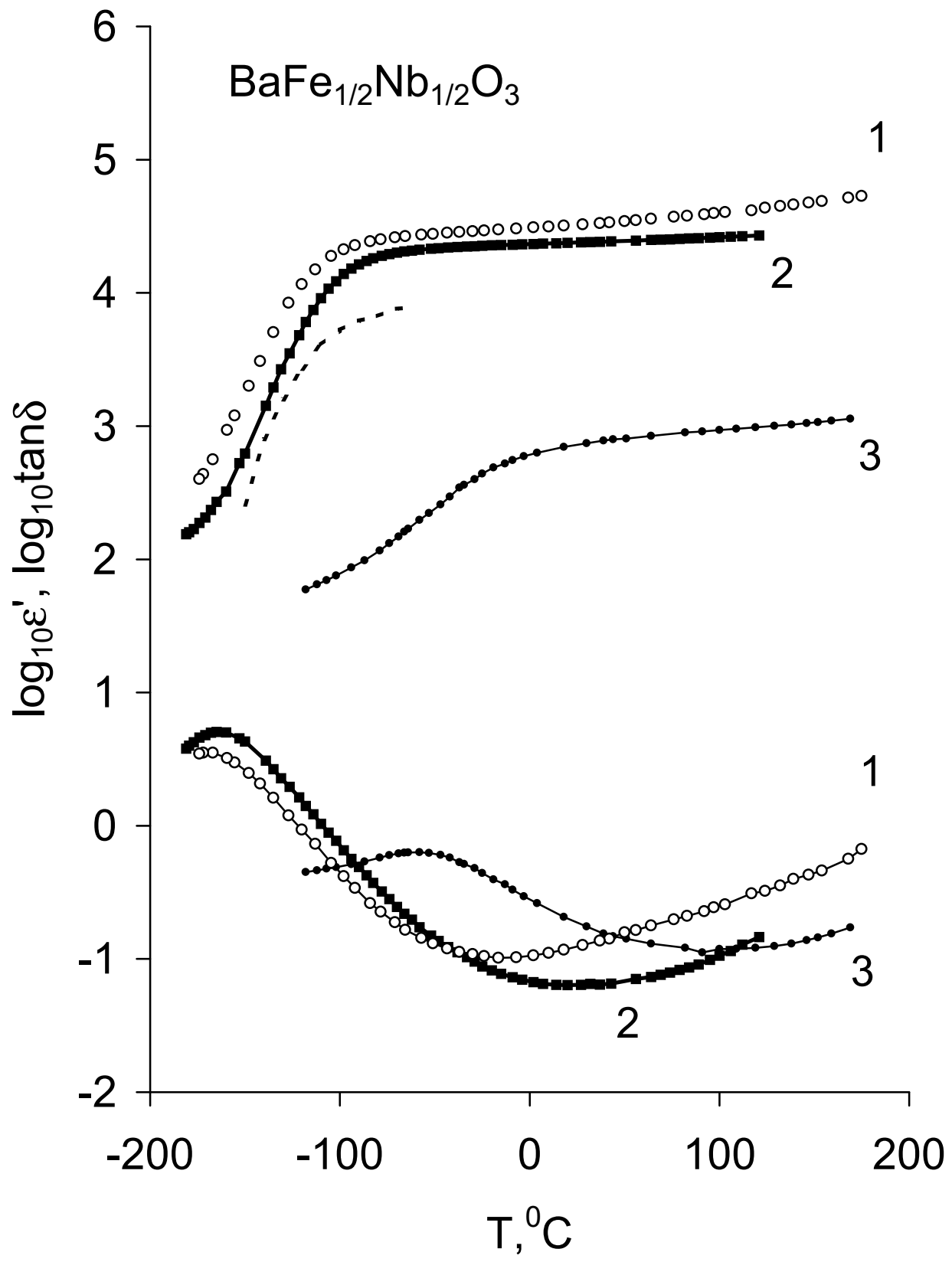
Fig. 3. Temperature dependencies of  $\varepsilon'$  (a),  $\tan\delta$  (b) and  $\varepsilon''$  (c) for BFN2 (filled symbols) and BFN3 (open symbols) measured at different frequencies.

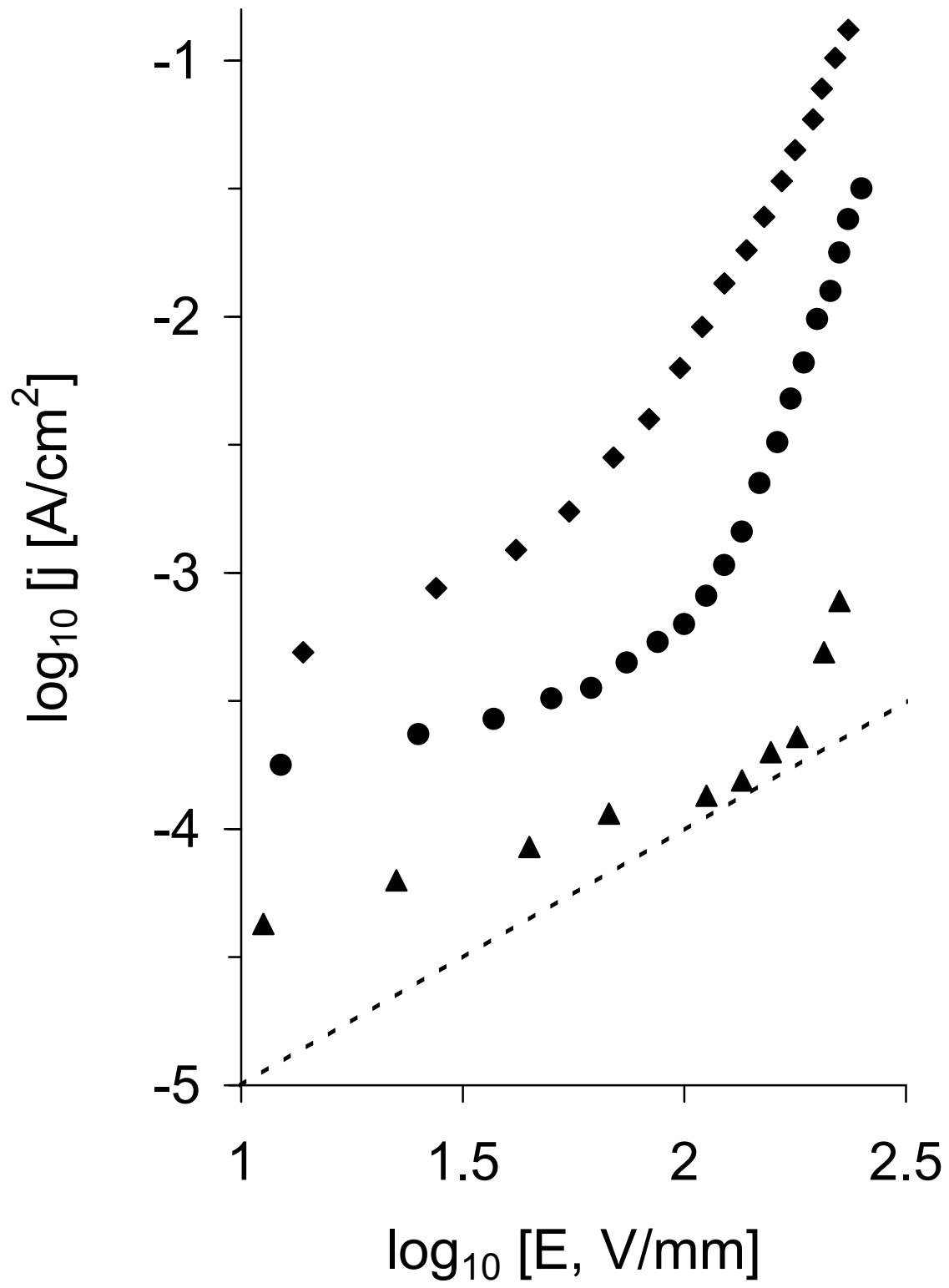
Fig. 4. The Arrhenius plots of the frequency dependence of the  $\tan\delta(T)$  maximum temperature (filled symbols) and  $\varepsilon''(T)$  maximum temperature (open symbols) for BFN-2 and BFN-3 ceramic samples having differing apparent resistivity values at room temperature. Symbols are the experimental points and solid lines are the least-squares straight-line fits.

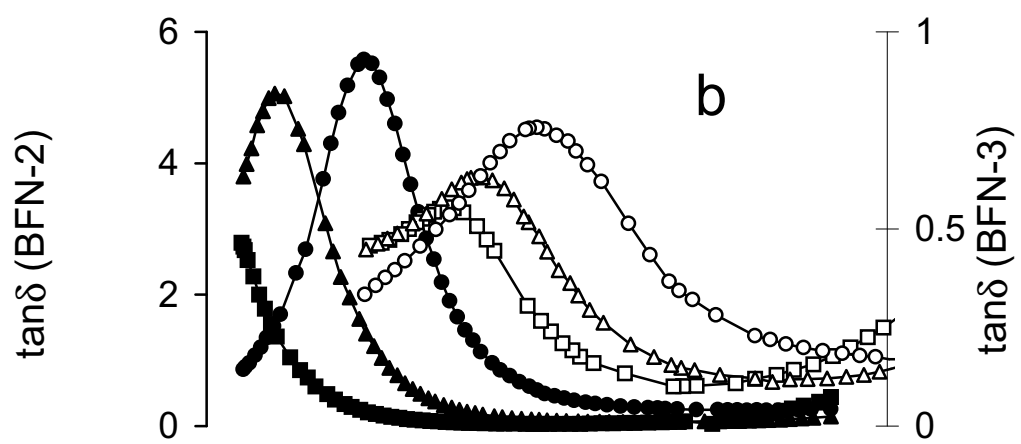
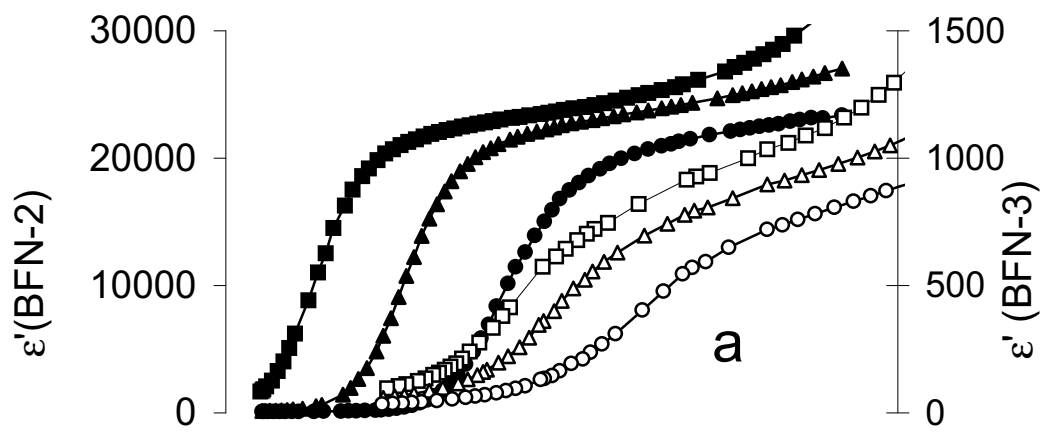
Fig. 5. Temperature dependencies of  $\varepsilon'$  (a) and  $\tan\delta$  (b) measured at 1 kHz for  $\text{BaFe}_{1/2}\text{Ta}_{1/2}\text{O}_3$  (1),  $\text{SrFe}_{1/2}\text{Nb}_{1/2}\text{O}_3$  (2),  $\text{CaFe}_{1/2}\text{Nb}_{1/2}\text{O}_3$  (3), and  $\text{SrFe}_{1/2}\text{Sb}_{1/2}\text{O}_3$  (4) ceramics.

Fig. 6. The Arrhenius plots of the frequency dependence of the  $\tan\delta(T)$  maximum temperature for  $\text{BaFe}_{1/2}\text{Ta}_{1/2}\text{O}_3$  (1),  $\text{SrFe}_{1/2}\text{Nb}_{1/2}\text{O}_3$  (2),  $\text{CaFe}_{1/2}\text{Nb}_{1/2}\text{O}_3$  (3), and  $\text{SrFe}_{1/2}\text{Sb}_{1/2}\text{O}_3$  (4) ceramics. Symbols are the experimental points and solid lines are the least-squares straight-line fits

Fig. 7. The fit of the Maxwell-Wagner theory to experiment on BFN-2.







■ 0,1kHz    ▲ 1kHz    ● 10kHz    □ 0,2kHz  
 ▲ 1kHz    ○ 10kHz

